RSC Advances

ROYAL SOCIETY
OF CHEMISTRY

www.rsc.org/advances

RSC Advances

RSC**Publishing**

ARTICLE

Determination of Particle Size Distribution of Water-Soluble CdTe Quantum Dots by Optical Spectroscopy

J.C.L. Sousa[a], M.G. Vivas[b,c], J.L. Ferrari[a], C.R. Mendonca[c], M.A. Schiavon[a]

In the present study, we report the synthesis of glutathione (GSH) capped CdTe quantum dots (QDs) using the one-pot approach as well as their optical properties. These QDs were used as a probe for a detailed quantitative correlation between spectroscopic data and QDs size dispersion. We have developed a spectroscopic method to determine the size dispersion of QDs in solution based on the fluorescence spectroscopy and the fluorescence quantum yields. Our results demonstrate that the one-pot approach produces GSH-capped CdTe QDs of narrow size dispersion, as inferred by the sharp line width (full width at half maximum) of the fluorescence signal (from 153 meV to 163 meV), as revealed by our spectroscopy method. We observed that the GSH-capped CdTe QDs cause an increase in fluorescence quantum yield from 11% to 30% concomitantly with an increase in lifetime decay from 38 to 50 ns during the course of synthesis (from 15 min to 120 min), indicating an increase in the average size of the QDs. Finally, we have used the evolving factor analysis together with the multivariate curve resolution-alternating least squares method to corroborate our results, and we found a good agreement between both methods with the advantage that in our method, we were able to obtain size dispersion rather than just the mean QD size.

Introduction

Colloidal semiconductor nanocrystals or quantum dots (QDs) are nanomaterials that exhibit a strong quantum confinement effect, which causes the appearance of size-dependent optical properties[1, 2]. Among these properties, we can cite high molar absorptivity[3, 4], high fluorescence quantum yield[5, 6], exceptional multiphoton absorption[7-11], and strong electron-phonon coupling[12, 13]. Because of these remarkable features, QDs are of great technological interest since they have been used in several applications, such as solar and photovoltaic cells[14, 15], luminescent biolabels[16], inkjet printing light-emitting devices[17], displays[18], and RGB devices[19, 20]. The production of high quality QDs with controllable physical and chemical properties is not trivial, and much effort has been devoted to develop useful synthetic approaches for producing high quality QDs. Among the synthetic routes for production of QDs, the liquid-phase approach has been proven as suitable for the fine-controlled synthesis of high quality QDs, when compared to vapour- and solid-phase approaches. QDs prepared by the liquid-phase approach can be dispersed in suitable solvents with the aid of capping organic molecules, termed surface ligands. These matrix-free QDs form stable suspensions that enable the direct application in solution-based techniques such as spin-coating, inkjet printing, and roll-to-roll casting[21].

Basically, the liquid-phase approach can be divided into two types: the aqueous-based approaches and nonaqueous-based approaches. The nonaqueous-approaches were first developed by employing organic solvents and organometallic precursors, which enables the fine-controlled synthesis of QDs. In this method, the particle sizes and shapes can be simply tailored by exploiting kinetically control over the nucleation and growth processes with the aid of organic ligands.[22, 23] In the past few decades, various non-aqueous methods have been developed, such as the hot-injection method,[24] and non-injection method[25]. On the other side, the aqueous-based approaches have the advantage of using environmentally friendly and biocompatible solvents, resulting in cheaper and greener synthesis processes.[26] However, these methods are usually incompatible with efficient size and morphology control of QDs due to the mild reaction temperatures.[27] Therefore, there has been an enormous effort in developing aqueous-based approaches, which are able in producing high quality QDs, with optical properties comparable with the ones obtained from nonaqueous-based approaches, and in developing methods of characterization of the optical, size and size distribution as well.

The synthesis of water-soluble CdTe QDs is routinely performed in two steps under an inert atmosphere by reducing tellurium powder with sodium borohydride.[2, 28] In order to reduce the complexity and consumption of materials, a tellurium precursor can be obtained by direct reduction of sodium tellurite in the presence of sodium borohydride under an ambient atmosphere. The best example described for this one-pot approach synthesis method of water-soluble CdTe QQs was the ones capped with L-glutathione (GSH), which showed strong staining and well-defined spectroscopy properties[29]. This method has been named the one-pot approach, and although it still requires further investigation for improvements, it seems to be a simpler method able to produce CdTe and others QDs as well.[30, 31]

With the development of these new methods of synthesis of water-

RSC Advances Accepted Manuscript

soluble QDs, it becomes very important to develop simpler and efficient methods for the optical characterization and determination of the size and size distribution of the QDs as well. Actually, a prerequisite to any application of QDs is that the QD absorption, emission and size-distribution properties are quantitatively understood. In this sense, the size-dependent optical properties of CdTe,[32, 33], CdSe, [32] CdS, [32] InAs,[34] and PbS [35] QDs have been previously reported. One of the most important physical features used to characterize synthesized colloidal QDs is determination of their average size and dispersion, which is generally, accomplished by high-resolution transmission electron microscopy (TEM). However, this technique is difficult to access, and moreover, requires very careful sample preparation to prevent nanoparticle agglomeration. In order to overcome such difficulties associated with TEM, other methods have been proposed to determine QDs size and size dispersion, including excitonic absorption peak measurements [32] and the study of size dispersion by spectroscopic and mathematical methods[28].

The most important work that correlates the optical properties with size determination of QDs was performed by Peng and co-authors [32]. The extinction coefficient per mole of nanocrystals at the first exitonic absorption peak, for high-quality CdTe, CdSe, and CdS nanocrystals was found to be strongly dependent on the size of the nanocrystals, between a square and a cubic dependence. The authors compiled TEM data and the maximum of the first excitonic absorption peak and find an empiric dependence useful for the determination of size and extinction coefficients of QDs. Mulvaney and cols [36] have re-examined the size-dependent optical absorption coefficients of CdSe nanocrystals at the band-edge, and established size dependent first absorption peak and molar extinction coefficient calibration curves, which can serve to accurately determine the concentration of nanocrystals in solution.

The first method developed to estimate the size of QDs based on their emission properties was reported by Radotic and co-authors [28]. As fluorescence spectroscopy is a simple and reliable methodology, which offers full spectral information it is possible to determine band position in fluorescence more precisely than in absorption spectra to estimate the size of both hydrophobic CdSe QDs and hydrophilic CdSe/ZnS QDs. The employment of evolving factor analysis (EFA) and multivariate curve resolution-alternating least squares (MCR-ALS) for decomposition of the series of QDs fluorescence spectra recorded by a specific measuring procedure revealed the number of quantum dot fractions having different diameters. The size of the quantum dots in a particular group was then defined by the fluorescence maximum position (FMP) of the corresponding component in the decomposed spectrum. However, no information regarding the size distribution of the QDs is obtained.

In this paper, we have developed a spectroscopic method to determine the mean size and also the size distribution of QDs in solution based on the fluorescence spectroscopy. In this method we have taken in account the absorbance and the fluorescence quantum yield and correlated these data for the GSH-capped CdTe QDs fractions through the simple numeric method. In addition, we measured the fluorescence quantum yield as a function of the CdTe QDs size to infer about the QDs quality obtained from the one-pot method. We have chosen the GSH-capped CdTe QDs since it is water-soluble and has been prepared by one of the simpler and greener methods described for this synthesis. Finally, we used EFA/MCR-ALS method to corroborate our results.

Experimental

Chemicals. $CdCl_2.H_2O$ (99%; Lot 0501337) was purchased from Vetec. L-Glutathione reduced (GSH; 98%; Lot SLBB3118V), $Na_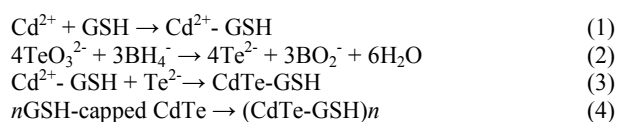2TeO_3$ (99%; Lot MKBG7198V), Rhodamine 101 (Lot 0001413183), and Rhodamine 6G (Lot 04718TH) were obtained from Sigma Aldrich. $NaBH_4$ (99%; Lot 0471BJH) was purchased from Fluka Analytical. All chemicals were used as received, without further purification. Mili-Q Water was used for experiments.

Synthesis of GSH-capped CdTe QDs. The experimental procedure used was based on a previously described paper [29]. Briefly, 0.4 mmol $CdCl_2.H_2O$ was diluted in 80 mL Mili-Q water in a 100 mL Beaker. GSH (0.52 mmol) was added while stirring, followed by adjusting the pH to 10.0 with a solution of 1.0 $molL^{-1}$ of NaOH. Next, this solution was added in a 100 mL three-neck flask with a reflux column and a thermocouple coupled with a thermal heater (Cole & Parmer®) in order to control the temperature. Then, 0.04 mmol Na_2TeO_3 and 1.0 mmol $NaBH_4$ were added to the solution, followed by reflux at 100 ±1ºC for up to 120 min. Aliquots were taken out at different time intervals and used to record the ultraviolet-visible (Uv-Vis) and photoluminescence (PL) spectra.

Characterization. Uv-Vis absorption and PL spectra were acquired on a Shimadzu Uv-2550 Spectrophotometer and Shimadzu RF-5301 PC fluorimeter, respectively. Absorption and fluorescence measurements were performed with 10 mm-quartz cuvettes (Shimadzu) using air-saturated solutions at room temperature. The fluorescence quantum yield (ϕ_f) of the nanocrystals was estimated by comparing the integrated emission of the QD samples obtained at one excitation wavelength, with that of a standard fluorescent dye (in this case Rhodamine 6G) [37]. We used the excitation wavelength of 355 nm. Essentially, stock solutions of the standard and QD samples with similar absorbance at the same excitation wavelength can be assumed to be absorbing the same number of photons. Hence, a simple ratio of the integrated fluorescence intensities of the two solutions (recorded under identical conditions) yielded the ratio of quantum yield values. Since the quantum yield for the standard sample Rhodamine 6G is known (ϕ_f = 0.95) in water [37, 38], it was trivial to calculate the quantum yield for the QDs. Identical instrument settings for sample and standard were used, and the solvent absorption and emission spectra were subtracted from the absorption and emission spectra of the sample and standard solutions. In addition, the measurements were repeated for at least five different sample and reference dye concentrations. Several syntheses of the GSH-capped CdTe were performed, and the ϕ_f measurements were determined at least three times, which allows the determination of the deviation standard of the ϕ_f for each synthesis time. The data processing routines was performed using the Evolving Factor Analysis (EFA) and multivariate curve resolution-alternating least squares (MCR-ALS) and the one proposed here were performed using MATLAB®, version 7.9.

Results and Discussion

The proposed mechanism of GSH-capped CdTe QDs formation is based on the route described by Wang and Liu [29]. However, these authors used thioglycolic acid as a stabilizing agent. Here, we propose a similar mechanism that uses GSH as a surface ligand, since this ligand has a strong appeal for biological systems applications. [39] Reactions 1 to 4 show the steps to GSH-capped CdTe QD formation.

$$Cd^{2+} + GSH \rightarrow Cd^{2+}\text{- GSH} \tag{1}$$
$$4TeO_3^{2-} + 3BH_4^- \rightarrow 4Te^{2-} + 3BO_2^- + 6H_2O \tag{2}$$
$$Cd^{2+}\text{- GSH} + Te^{2-} \rightarrow CdTe\text{-GSH} \tag{3}$$
$$n\text{GSH-capped CdTe} \rightarrow (CdTe\text{-GSH})n \tag{4}$$

Reaction 1 describes formation of the cadmium complex with glutathione ligand after pH adjustment. In reaction 2, tellurite was

reduced to telluride by borohydride. As telluride anion formed, it interacted with the cadmium complex to form QDs (reaction 3), and reached equilibrium through Ostwald Rippening process (reaction 4).

Figure 1(a) shows the absorption spectra of GSH-capped CdTe QDs at different synthesis times. According to Figure 1, the spectra were characterized by one well-defined absorption band that was assigned to the first excitonic transition ($1S_e \rightarrow 1S_{3/2}$), which was a function of QD size[2, 40]. Figure 1(b) displays fluorescence spectra of GSH-capped CdTe QDs excited at 355 nm. As can be seen, both absorption and fluorescence spectra shifted to longer wavelengths during the course of the synthesis, due to the increase in the average size of the QDs. This increase in size is typical of colloidal synthesis, regardless of the method used for QD production[39]. Furthermore, the sharp line width (full width at half maximum; FWHM) for both absorption and fluorescence spectra were sharp, indicating that this method produced GSH-capped CdTe QDs of narrow size dispersion[29, 30]. Such physical parameters are of major importance in determining the electronic and optical features of QDs, as well in choosing their most appropriate application.
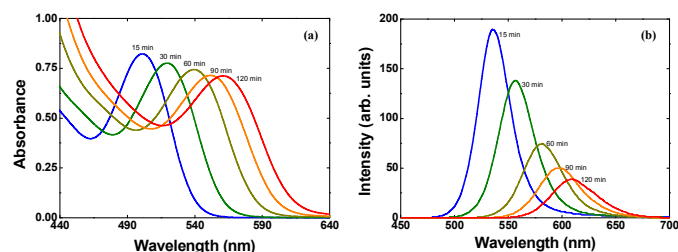

Figure 1. Evolution of GSH-capped CdTe solution absorption (a) and fluorescence (b) spectra with the synthesis time.

Another important aspect to highlight in Figure 1(b) is the fact that the fluorescence intensity decreased with an increase in synthesis time. Based on the Beer's Law (C=A/Lε(D), where A is the absorbance, L the optical length) and the empirical correlation obtained by Yu et al.[32] between molar absorptivity (ε) and diameter (D), the concentration decreased from 13.1 μM at 15 min to 5.5 μM at 120 min. Therefore, the result of Fig. 1(b) can be explained, at least in part, by a decrease in QD concentration due to the increase in the atom number necessary to generate QDs with larger diameters.

As a first approach to determining QD size, we used the empirical correlation between the first absorption peak and the QD size found by Yu et al.[32], as previously described. After that, we correlated the QDs size with the fluorescence maximum position, as shown in Fig. 2. It is worth mentioning that this procedure is very important to the determination of QDs size dispersion (as will be shown later), since the fluorescence spectrum is much more sensible to the increase of the QD size than the absorption peak. Figure 2 displays the relation between the QD size and fluorescence maximum position. It was observed that QD growth kinetics exhibited exponential behavior, with a R^2 coefficient of 0.9999, indicating an excellent fit. This behavior is typical of colloidal synthesis. One of the most interesting optical properties of QDs is their high fluorescence quantum yield (ϕ_f). Thus, we estimated the fluorescence quantum yield for CdTe-GSH QDs dissolved in water using rhodamine 6G [37] as a standard with a previously described methodology [38]. The ϕ_f of rhodamine 6G was checked by using the rhodamine 101, which has ϕ_f of 100% (Figure S1 in Supplementary Information). The GSH-capped CdTe fluorescence quantum yields for different synthesis times are shown in Figure 3. As it can be seen, fluorescence quantum yields reached a maximum of 30% at 60 min, with little change to this value when the synthesis time increased to 120 min.
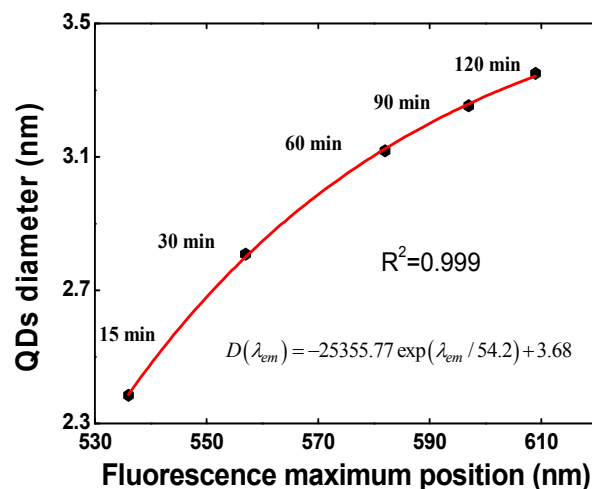

Figure 2. Size/FMP dependence for GSH-capped CdTe QDs.

The fluorescence quantum yield values obtained were within the range of those reported in the literature for CdTe nanocrystals synthesized in aqueous media [26, 41, 42]. A typical calibration curve for the ϕ_f is shown if Figure S2 (Supplementary Information). The solid line in Figure 3 represents the fitting curve used to model ϕ_f for CdTe QDs with different sizes, which will be subsequently used to evaluate the size dispersion of the QDs in solution. It is observed that the fluorescence quantum yield has a sigmoidal behaviour with the increase of QDs size. In general, but not as a rule, the fluorescence quantum yield increase with the increase of the QD size (as observed to the synthesis times between 15 and 60 minutes) and, after that, this value tends to remain constant within experimental error (60 to 120 minutes). However, with the considerable increase of QDs diameter (higher than 3.5 nm) the number of defects on their surface tends to increase and, as consequence, the fluorescence quantum yield inclines to decrease as reported in Ref.[39] for GSH-CdTe QDs.
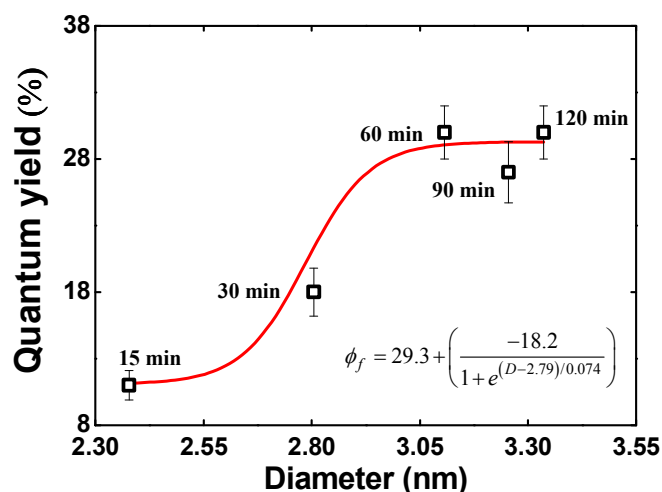

Figure 3. GSH-capped CdTe fluorescence quantum yield versus average diameter.

Another important feature related to the size of the QDs is the fluorescence lifetime. Here, this parameter was measured using a 70-ps laser at 532 nm as an excitation source (second harmonic of a Q-switched and mode-locked Nd:YAG laser) operating at a 100 Hz repetition rate. Details about the experimental setup and the

convolution method used to fit the lifetime decay were previously described [43, 44]. It is important to mention that all fluorescence decay curves of excitonic emission from GSH-capped CdTe QDs were fitted using a single-exponential function. As can be seen in Figure 4, the fluorescence lifetimes for the GSH-capped CdTe QDs synthesized by the one-pot approach increased with synthesis time (or size); namely, from 38.5 ns at 15 min to 50 ns at 120 min. A plausible explanation for this result is because larger QDs have more spaced energy levels, the probability of trapping electron-hole pairs is increased, and therefore, the lifetime will be longer [45].
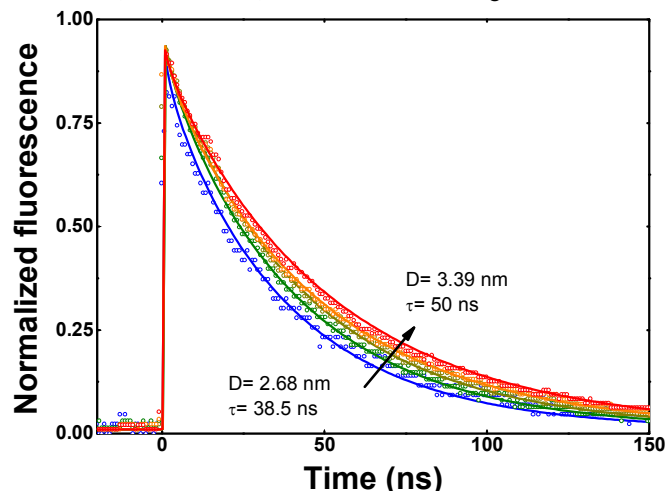

Figure 4. Fluorescence lifetimes (τ = 38.5; 41.5; 44.0; 47.5; 50.0 ns) for the GSH-capped CdTe QDs synthesized by one-pot approach.

In general, CdTe QDs with sizes between 2.5 to 3.5 nm have fluorescence lifetimes from 15 to 30 ns [45-48], depending on the synthesis method and stabilizing agent used. However, our results showed longer lifetimes, which may be indicative that the surface quality of the nanoparticles is improved by reducing defects. From the point of view of imaging applications, longer fluorescence lifetimes allow better discrimination of the signal from cellular auto fluorescence and scattered excitation light, thereby yielding better image quality [49, 50].

As previously mentioned, determination of QD size dispersion requires sophisticated techniques such as TEM, which require very careful sample preparation to avoid its agglomeration. Therefore, to overcome such difficulties, we showed that is possible to obtain a good estimative of QD size dispersion through the fluorescence spectra, excited at several wavelengths along the first excitonic band. In Figure 5 we show the flow diagram that illustrates the method we developed to determine the size dispersion from the spectroscopic data. Initially, we measured the fluorescence spectra after stepwise excitation (intervals of 5 nm) at several wavelengths along the lowest energy excitonic band of the QDs. These data were placed in a M (n,m) matrix, where n corresponded to the excitation wavelength and m corresponded to the component spectra (i.e., intensity values provided by the fluorimeter).

The corresponding wavelength range of the fluorescence spectra were stored in the vector W(m). To remove possible contributions of Rayleigh scattering in the fluorescence spectra, we used a linear filter ("Filter routine" in the diagram of Fig. 5).
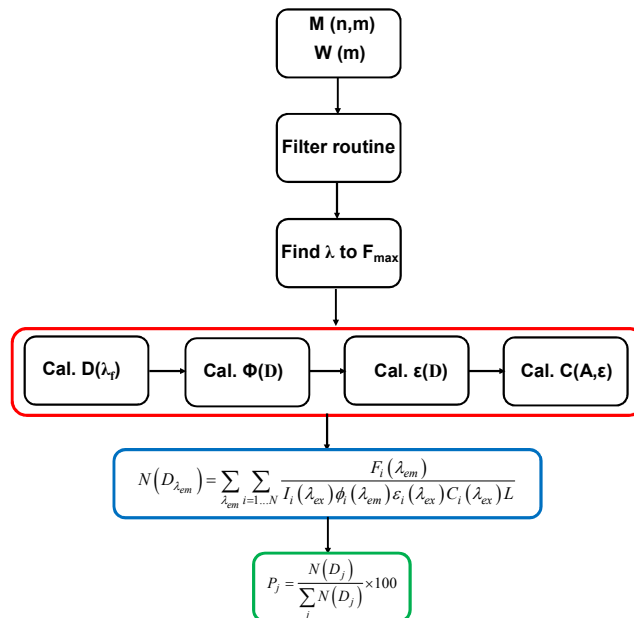

Figure 5. Flow diagram used to explain the method employed to determine the size dispersion through the spectroscopic data.

Figure 6 shows an illustrative graph (colormap) of the excitation versus emission wavelengths. The deep blue line displays the filter used to remove Rayleigh scattering in the fluorescence spectra.
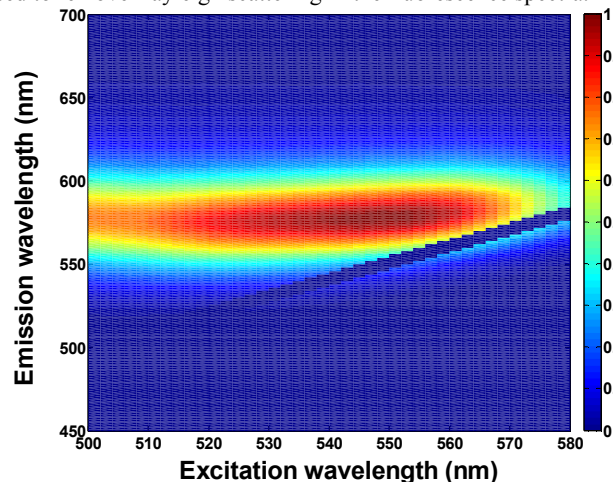

Figure 6. Colormap representing the graph of the excitation versus emission wavelengths to the synthesis time of 60 min.

Subsequently, we determined the wavelength corresponding to the fluorescence spectra peak ("Find λ to F_{max}" in the diagram). The fluorescence spectra obtained by exciting the QDs in different wavelength along the first excitonic band are showed in Figure S3 (Supplementary information) for the sample obtained after 30 minutes of synthesis. By substituting these results in the equation obtained through Figure 2, we obtained the values of QD diameters in ensemble. Thus, we calculated the QD fluorescence quantum yield, the molar absorptivity, and concentration using the calibration curve (Fig. 3), the empirical relationship obtained by Yu *et al.* [32] and Beer's Law, respectively. Finally, we determined the percentage of QDs with a specific diameter using:

$$P_j = \frac{N(D_j)}{\sum_j N(D_j)} \times 100$$

with,

$$N(D_{\lambda_{em}}) = \sum_{\lambda_{em}} \sum_{i=1...N} \frac{F_i(\lambda_{em})}{I_i(\lambda_{ex})\phi_i(\lambda_{em})\varepsilon_i(\lambda_{ex})C_i(\lambda_{ex})L}$$

where P_j was the percentage of QDs with a specific diameter present in ensemble, $F_i(\lambda_{em})$ was the maximum fluorescence intensity, I was the intensity of the excitation wavelength (xenon lamp), $\phi(\lambda_{em})$ and $\varepsilon(\lambda_{ex})$ were the fluorescence quantum yield and molar absorptivity, respectively for the QD with diameters corresponding to the excitation wavelength, and L was the optical length. The summation on i was performed to add QDs with the same diameter contained in ensemble. The algorithm developed can be found in "Electronic Supplementary Information". The bars in Figure 7 show the size dispersion for GSH-capped CdTe QDs obtained through the method described in Figure 5, while the solid lines are the lognormal fit used to model the size dispersion.
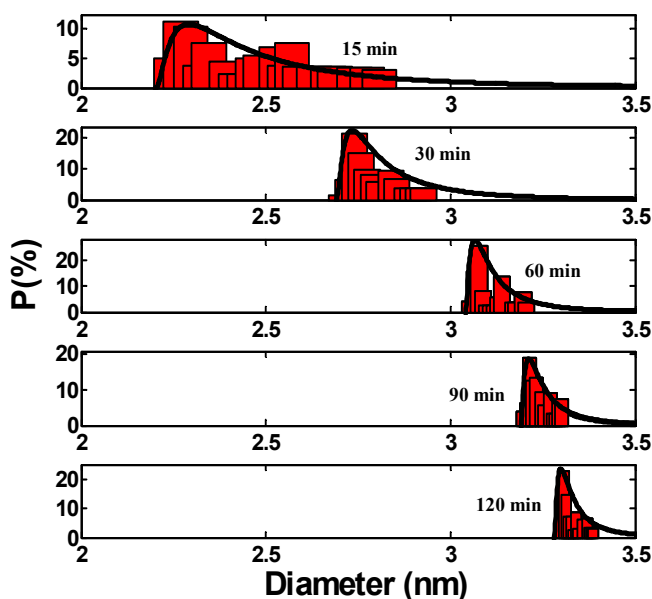

Figure 7. The bars present the size dispersion for CdTe QDs obtained through the method described in the diagram of Figure 5, while the solid lines are the lognormal fit used to model the size dispersion.

It was observed that the size dispersion decreased with synthesis time (from 15 to 120 min) while the average size increased. Moreover, no particles with sizes larger than 1.5 times the average size were present in ensemble. This is a particular behavior of the Ostwald Ripening mechanism [51, 52], in which increasing synthesis time causes smaller QDs to dissolve and precipitate onto the surface of larger QDs. As a consequence, the average QD size increases and its variance decreases [31]. To corroborate these results, we compared our method with the EFA/MCR-ALS method [53]. Based on this method, the characteristic emission spectra of a QD ensemble was obtained calculating successively, in an iterative process, the eigenvalues generated by emission spectra excited along the first excitonic band. Details about this method can be found elsewhere [28, 53]. Some illustrative results obtained from this method are reported in Figures S4 and S5 (Supplementary information). Normalized emission spectra obtained from the EFA/MCR-ALS routine for each

synthesis time are depicted in Figure 8. According to EFA/MCR-ALS analysis, the QD diameter predominant in the ensemble were 2.37 and 2.51 nm for 15 min, 2.72 and 2.84 nm for 30 min, 3.05 and 3.15 nm for 60 min, 3.21 and 3.27 nm for 90 min, and 3.29 and 3.36 nm for 120 min. As it can be seen, the main diameters obtained from the EFA/MCR-ALS analysis were also obtained with the method we proposed.
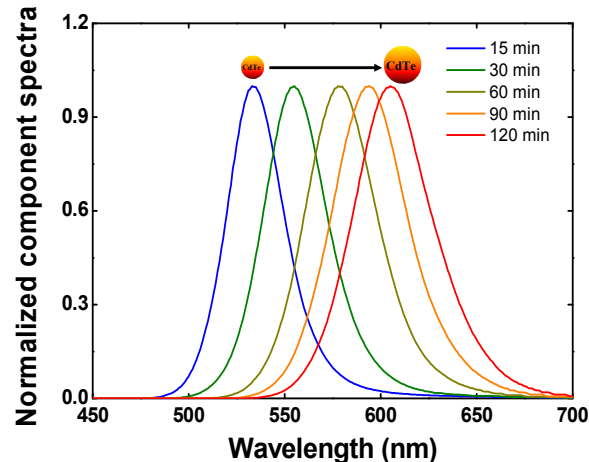

Figure 8. Normalized characteristic emission spectra obtained from the EFA/MCR-ALS method for each QDs solution.

Conclusions

In this report, we studied the optical properties of GSH-capped CdTe QDs synthesized by the one-pot approach, and use it as probe to determination of size and size dispersion in our method. This one-pot approach method has the advantage, compared with the organic-based approaches, of being performed in an aqueous medium, which reduces the cost, decreases the environmental impacts, and increases reproducibility. Our results showed that the one-pot approach produces GSH-capped CdTe QDs of similar high quality and more narrow size dispersion as those produced using an organic route. [54] The longer fluorescence decay lifetime observed for the GSH-capped CdTe QDs synthesized by the one-pot approach, compared with other methods, was attributed to the improve in surface quality of the nanoparticles by reducing defects. Fluorescence quantum yields between 11% and 30% were observed for the GSH-capped CdTe QDs with diameters from 2.3 to 3.5 nm, which was in accordance with other synthesis methods. By using the spectroscopic method proposed here, which was based on the fluorescence of QDs, it was possible to show that during the course of the one-pot synthesis, the size dispersion of QDs in solution decreased and had a lognormal dispersion. Furthermore, based on this method, the size dispersion of QDs in solution was narrow since in solution and at low concentration the QDs agglomeration is practically negligible and, therefore, QDs have a much higher free volume (filling factor). Moreover, during the one-pot synthesis occurs the dissolution of the smaller QDs, that are less stable, and the precipitation of them on the larger QDs (Ostwald ripening)[38] decreasing, thereby, the size dispersion. Finally, we used EFA/MCR-ALS analysis and found a good agreement between both methods with the advantage that in our method, we were able to obtain size dispersion rather than just the main QD size.

Acknowledgements

Notes and references

[a] Grupo de Pesquisa em Química de Materiais (GPQM), Departamento de Ciências Naturais, Universidade Federal de São João del-Rei, 74, 36301-160, São João del-Rei, MG, Brazil

[b] Instituto de Ciência e Tecnologia, Universidade Federal de Alfenas, Cidade Universitária - BR 267 Km 533, 37715-400, Poços de Caldas, MG, Brazil

[c] Instituto de Física de São Carlos, Universidade de São Paulo, Caixa Postal 369, 13560-970 São Carlos, SP, Brazil

Electronic Supplementary Information (ESI) available: [Calibration curves for the determination of fluorescence quantum yields of GSH-CdTe QDs; set of PL spectra excited at different wavelengths; Graphics from EFA/MCR-ALS analysis and the algorithm to the determination of QDs size dispersion]. See DOI: 10.1039/b000000x/

1   A. P. Alivisatos, *Science*, 1996, 271, 933-937.
2   A. L. Rogach, *Semiconductor Nanocrystal Quantum Dots: Synthesis, Assembly, Spectroscopy and Application*, Springer, NewYork, 2008.
3   J. Sun and E. M. Goldys, *Journal of Physical Chemistry C*, 2008, 112, 9261-9266.
4   I. Moreels, K. Lambert, D. Smeets, D. De Muynck, T. Nollet, J. C. Martins, F. Vanhaecke, A. Vantomme, C. Delerue, G. Allan and Z. Hens, *Acs Nano*, 2009, 3, 3023-3030.
5   W. C. W. Chan and S. M. Nie, *Science*, 1998, 281, 2016-2018.
6   X. Michalet, F. F. Pinaud, L. A. Bentolila, J. M. Tsay, S. Doose, J. J. Li, G. Sundaresan, A. M. Wu, S. S. Gambhir and S. Weiss, *Science*, 2005, 307, 538-544.
7   M. G. Vivas, J. F. Cury, M. A. Schiavon and C. R. Mendonca, *Journal of Physical Chemistry C*, 2013, 117, 8530-8535.
8   J. Szeremeta, M. Nyk, D. Wawrzynczyk and M. Samoc, *Nanoscale*, 2013, DOI: 10.1039/C3NR33860F.
9   L. A. Padilha, G. Nootz, P. D. Olszak, S. Webster, D. J. Hagan, E. W. Van Stryland, L. Levina, V. Sukhovatkin, L. Brzozowski and E. H. Sargent, *Nano Letters*, 2011, 11, 1227-1231.
10   S.-C. Pu, M.-J. Yang, C.-C. Hsu, C.-W. Lai, C.-C. Hsieh, S. H. Lin, Y.-M. Cheng and P.-T. Chou, *Small*, 2006, 2, 1308-1313.
11   Y. Qu and W. Ji, *Journal of the Optical Society of America B-Optical Physics*, 2009, 26, 1897-1904.
12   K. J. Williams, W. A. Tisdale, K. S. Leschkies, G. Haugstad, D. J. Norris, E. S. Aydil and X. Y. Zhu, *Acs Nano*, 2009, 3, 1532-1538.
13   S. Hameau, Y. Guldner, O. Verzelen, R. Ferreira, G. Bastard, J. Zeman, A. Lemaitre and J. M. Gerard, *Physical Review Letters*, 1999, 83, 4152-4155.
14   E. H. Sargent, *Nature Photonics*, 2012, 6, 133-135.
15   C.-H. Chang and Y.-L. Lee, *Applied Physics Letters*, 2007, 91.
16   W. C. W. Chan, D. J. Maxwell, X. H. Gao, R. E. Bailey, M. Y. Han and S. M. Nie, *Current Opinion in Biotechnology*, 2002, 13, 40-46.
17   H. M. Haverinen, R. A. Myllyla and G. E. Jabbour, *Applied Physics Letters*, 2009, 94.
18   K. Bourzac, *Nature*, 2013, 493, 283-283.
19   S. Coe-Sullivan, J. S. Steckel, L. A. Kim, M. G. Bawendi and V. Bulovic, in *Light-Emitting Diodes: Research, Manufacturing, and Applications IX*, eds. S. A. Stockman, H. W. Yao and E. F. Schubert, 2005, vol. 5739, pp. 108-115.
20   P. O. Anikeeva, J. E. Halpert, M. G. Bawendi and V. Bulovic, *Nano Letters*, 2009, 9, 2532-2536.
21   J. Y. Kim, O. Voznyy, D. Zhitomirsky and E. H. Sargent, *Advanced Materials*, 2013, 25, 4986-5010.
22   Y. Yin and A. P. Alivisatos, *Nature*, 2005, 437, 664-670.
23   E. A. Weiss, *Accounts of Chemical Research*, 2013, 46, 2607-2615.
24   C. B. Murray, D. J. Norris and M. G. Bawendi, *Journal of the American Chemical Society*, 1993, 115, 8706-8715.
25   W. Zhang, H. Zhang, Y. Feng and X. Zhong, *Acs Nano*, 2012, 6, 11066-11073.
26   F. O. Silva, M. S. Carvalho, R. Mendonca, W. A. A. Macedo, K. Balzuweit, P. Reiss and M. A. Schiavon, *Nanoscale Research Letters*, 2012, 7.
27   Z. Zhuang, Q. Peng and Y. Li, *Chemical Society Reviews*, 2011, 40, 5492-5513.
28   D. Mutavdzic, J. Xu, G. Thakur, R. Triulzi, S. Kasas, M. Jeremic, R. Leblanc and K. Radotic, *Analyst*, 2011, 136, 2391-2396.
29   Y. Wang and S. Liu, *Journal of the Chilean Chemical Society*, 2012, 57, 1109-1112.
30   Y. Zhu, Z. Li, M. Chen, H. M. Cooper, G. Q. Lu and Z. P. Xu, *Journal of Colloid and Interface Science*, 2013, 390, 3-10.
31   G. W. Huang, C. Y. Chen, K. C. Wu, M. O. Ahmed and P. T. Chou, *Journal of Crystal Growth*, 2004, 265, 250-259.
32   W. W. Yu, L. H. Qu, W. Z. Guo and X. G. Peng, *Chemistry of Materials*, 2003, 15, 2854-2860.
33   A. M. Funston, J. J. Jasieniak and P. Mulvaney, *Advanced Materials*, 2008, 20, 4274-4280.
34   P. R. Yu, M. C. Beard, R. J. Ellingson, S. Ferrere, C. Curtis, J. Drexler, F. Luiszer and A. J. Nozik, *Journal of Physical Chemistry B*, 2005, 109, 7084-7087.
35   L. Cademartiri, E. Montanari, G. Calestani, A. Migliori, A. Guagliardi and G. A. Ozin, *Journal of the American Chemical Society*, 2006, 128, 10337-10346.
36   J. Jasieniak, L. Smith, J. van Embden, P. Mulvaney and M. Califano, *Journal of Physical Chemistry C*, 2009, 113, 19468-19474.
37   R. F. Kubin and A. N. Fletcher, *Journal of Luminescence*, 1982, 27, 455-462.
38   J. N. Demas and G. A. Crosby, *Journal of Physical Chemistry*, 1971, 75, 991-1024.
39   Y. Zheng, S. Gao and J. Y. Ying, *Advanced Materials*, 2007, 19, 376-380.
40   A. D. Yoffe, *Advances in Physics*, 2001, 50, 1-208.
41   M. Grabolle, M. Spieles, V. Lesnyak, N. Gaponik, A. Eychmueller and U. Resch-Genger, *Analytical Chemistry*, 2009, 81, 6285-6294.
42   Y.-h. Zhang, H.-s. Zhang, M. Ma, X.-f. Guo and H. Wang, *Applied Surface Science*, 2009, 255, 4747-4753.
43   M. G. Vivas, S. L. Nogueira, H. S. Silva, N. M. B. Neto, A. Marletta, F. Serein-Spirau, S. Lois, T. Jarrosson, L. De Boni, R. A. Silva and C. R. Mendonca, *Journal of Physical Chemistry B*, 2011, 115, 12687-12693.
44   M. G. Vivas, D. L. Silva, L. De Boni, Y. Bretonniere, C. Andraud, F. Laibe-Darbour, J. C. Mulatier, R. Zalesny, W. Bartkowiak, S. Canuto and C. R. Mendonca, *Journal of Physical Chemistry B*, 2012, 116, 14677-14688.
45   A. F. van Driel, G. Allan, C. Delerue, P. Lodahl, W. L. Vos and D. Vanmaekelbergh, *Physical Review Letters*, 2005, 95.
46   Yong, K.T., Law, W.C., Roy, I., Jing, Z., Huang, H., Swihart, M. T., Prasad, P. N., *Journal of biophotonics*, 2011, 4, 9-20.
47   Hines, D. A., Kamat, P. V., *Applied Materials and Interfaces*, 2014, 6, 3041-3057.
48   Petryayeva, E., A lgar, W. R., Medintz, I. L., *Applied Spectroscopy*, 2013 67, 60-88.
49   U. Resch-Genger, M. Grabolle, S. Cavaliere-Jaricot, R. Nitschke and T. Nann, *Nature Methods*, 2008, 5, 763-775.
50   M. Dahan, T. Laurence, F. Pinaud, D. S. Chemla, A. P. Alivisatos, M. Sauer and S. Weiss, *Optics Letters*, 2001, 26, 825-827.
51   R. D. Vengrenovich, Y. V. Gudyma and S. V. Yarema, *Semiconductors*, 2001, 35, 1378-1382.
52   R. Finsy, *Langmuir*, 2004, 20, 2975-2976.
53   H. R. Keller and D. L. Massart, *Chemometrics and Intelligent Laboratory Systems*, 1992, 12, 209-224.
54   C. Ge, M. Xu, J. Liu, J. Lei and H. Ju, *Chemical Communications*, 2008, DOI: 10.1039/b714990e, 450-452.